

Implementation and Simulation of Hovering Control Model for Flapping Wing Aircraft

Qifan Zhang¹, Xia Jiang²

¹Faculty of Information Science and Engineering, China University of Petroleum-Beijing, Beijing, 102249, China

²Faculty of Automation and Electrical Engineering, Tianjin University of Technology and Education, Tianjin, China

Abstract: In recent years, bionic flapping wing aircraft is widely used in battlefield reconnaissance and flight patrol, making it a popular research in the field of UAV. However, because the wing and body forces are complex and conventional method calculation and modeling are difficult, so it is urgent to study the flight control of flapping aircraft. In this paper, the rigid body dynamics modeling method is used firstly to analyze the wing motion, establish the dynamic model of the wing aircraft, and then the PID control model is used to control the suspended motion state of the wing aircraft, and at last control simulation using Simulink. The results show that the mean value of the angular velocity fluctuation with PID control is 32.6% of the value without control, and the change rate is 38.2% of the value without control. The attitude adjustment process is more stable and the performance is better.

Keywords: Flapping wing aircraft; Angular speed; Attitude Angle; PID

1. Introduction

With a long history, dating back to Daedalus in ancient Greece, flapping wing aircraft has many advantages over fixed-wing aircraft, such as power system and control system; higher mechanical efficiency than fixed-wing aircraft, making its research and manufacturing a relatively hot field and subject recently.

At present, the cutting-edge research includes: the hummingbird flight robot in the United States has a camera system that can realize tilt, rolling and rotation multidimensional control, but the system is low and it is difficult to cope with complex task requirements.

The Harvard Wood team has developed a flying insect robot with a microprocessed intelligent composite microstructure, increasing wing load capacity by 300% but increasing energy loss by only 55%. However, it is still inadequate and has poor control; the DelFly II has a carbon skeleton and lighter elements such as brushless motors; the H2bird Microwing of Berkeley, with a carbon fiber structure and greater flexibility.

China's research on flapping aircraft is also at the forefront of the world. The ASN-211 flapping aircraft personnel of Northwest China University of Technology in China, equipped with micro cameras, can take off independently, has strong wind resistance, and can be used for a variety of mission activities [1].

However, the dynamic modeling of the flapping wing aircraft itself has complex models, many restrictive factors, and complex force points and complex disturbances to be considered, which makes it difficult to study its suspension and forward fields. According to the above problems, this

Paper simplifies the stress model and establishes the model of dynamic simulation. Controlling the balance and stability of the plane angle speed of the plane, modify PID parameters and optimize the angular velocity and the rate of change.

2. Theoretical mechanical modeling of flapping wing aircraft

The posture of insects are significantly affected by their movement and force during flight. In order to describe the movement posture of insects, the Euler angle of insect movement posture is introduced, that is Euler(ϕ, θ, φ).

ϕ is the yaw angle, that is, the angle between the projection of the vertical axis y in the horizontal plane and the y -axis. θ is the pitch angle, the angle between the vertical axis y and the horizontal plane. φ is the tumbling angle, the angle between the symmetric plane of the insect and the lead hammer plane passing through the longitudinal axis y . Euler(ϕ, θ, φ) shows the attitude motion equation of the insect, whose angular velocity ω is represented by the attitude angle of the insect. Finally, the equation of posture motion can be derived. The attitude angle is described in Fig.1 below.

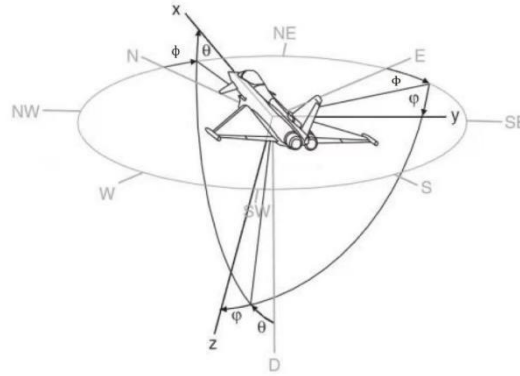


Figure 1: Position and motion diagram of the flying vehicle

$$\omega_x = \dot{\phi} \sin \theta \sin \varphi + \dot{\theta} \cos \varphi \quad (1)$$

$$\omega_y = \sin \theta \sin \varphi - \dot{\theta} \sin \varphi \quad (2)$$

$$\omega_z = \dot{\phi} + \dot{\phi} \cos \theta \quad (3)$$

The equations for the force in each direction of the wing wingspan are:

$$F_N = \frac{1}{2} c_N(u, v, w) \rho U^2 S \quad (4)$$

$$F_C = \frac{1}{2} c_C(u, v, w) \rho U^2 S \quad (5)$$

$$F_S = \frac{1}{2} c_S(u, v, w) \rho U^2 S \quad (6)$$

In the above formula, F_N , F_C and F_S are three aerodynamic components in the wing plane frame, S is the wing area. And c_N, c_C, c_S are the normal, string and spreading, respectively; $\mu(\xi, \psi, \zeta)$ is the angular vector of wing motion, $v(v_x, v_y, v_z)$ is the velocity vector of the aircraft, $\omega(\phi, \theta, \varphi)$ is the attitude vector, ρ is air density and U is the reference velocity. The coordinate system is now the wing coordinate system.

Component moments on each wing are expressed as:

$$M_L = \frac{1}{2} c_L(u, v, w) \rho U^2 S c \quad (7)$$

$$M_M = \frac{1}{2} c_M(u, v, w) \rho U^2 S c \quad (8)$$

$$M_N = \frac{1}{2} c_N(u, v, w) \rho U^2 S c \quad (9)$$

In the formula(7)-(9), M_L, M_M and M_N are the three components of the aerodynamic moment in the wing plane frame; S is the wing area; c_L, c_M and c_N are the wing normal, string, and spreading aerodynamic torque factors, respectively; $\mu(\xi, \psi, \zeta)$ is the angular vector of the wing movement. $v(v_x, v_y, v_z)$ is the speed vector of the flying vehicle; $\omega(\phi, \theta, \varphi)$ is the pose vector. ρ is the air density; U is the reference speed; The c is the average string length; The coordinate system is now the wing coordinate system.

Also transform the coordinates in the later operation:

The forces and moments in the wing frame can be transformed into the forces in the insect body frame by the coordinate rotation transformation, which can be expressed as:

$$F_B = T_B(F_C, F_S, F_N)^T \quad (10)$$

T_B can be represented as:

$$T_B(\xi, \phi, \zeta) = \begin{bmatrix} \cos\xi\cos\phi & \cos\xi\sin\phi\sin\zeta & \cos\xi\sin\phi\cos\zeta + \sin\xi\sin\zeta \\ \sin\xi\cos\phi & \sin\xi\sin\phi\sin\zeta & \sin\xi\sin\phi\cos\zeta - \cos\xi\cos\zeta \\ -\sin\phi & \cos\phi\sin\xi & \cos\phi\sin\xi \end{bmatrix} \quad (11)$$

Under the inertial frame system, it can be expressed as:

$$F_1 = T_1 F_B \quad (12)$$

And:

$$M_B = T_B(M_L, M_M, M_N)^T \quad (13)$$

$$M_1 = T_1 M_B \quad (14)$$

The combined external force that insects receive during flight can be expressed as:

$$F^I = F_r^W + F_l^W + F^B + F^G \quad (15)$$

In the formula, F_r^W and F_l^W are the force of the insect left and right wing, and F^G is the insect body force.

The resultant moment can be expressed as:

$$M^I = M_r^W + M_l^W + M^B \quad (16)$$

M_r^W, M_l^W, M^B are shown as the moment and physical distance between the left and right wings of insects.

Meanwhile, the pose dynamics equation of the vehicle body in 3D space is:

$$M_x = I_x \frac{d\omega_x}{dt} + \omega_y \omega_z (I_z - I_y) \quad (17)$$

$$M_y = I_x \frac{d\omega_x}{dt} + \omega_x \omega_z (I_x - I_z) \quad (18)$$

$$M_z = I_z \frac{d\omega_x}{dt} + \omega_x \omega_y (I_y - I_x) \quad (19)$$

The upper equation is the attitude dynamics equation of the Kun flapping wing aircraft, in which, respectively, I_x, I_y and I_z are the rotary inertia of the insect wing around the coordinate axis. From the relationship between rotation angle velocity and attitude angle, and the insect pose angle [2].

3. Simulation and result analysis

The flow chart of our entire modeling process is as follows:

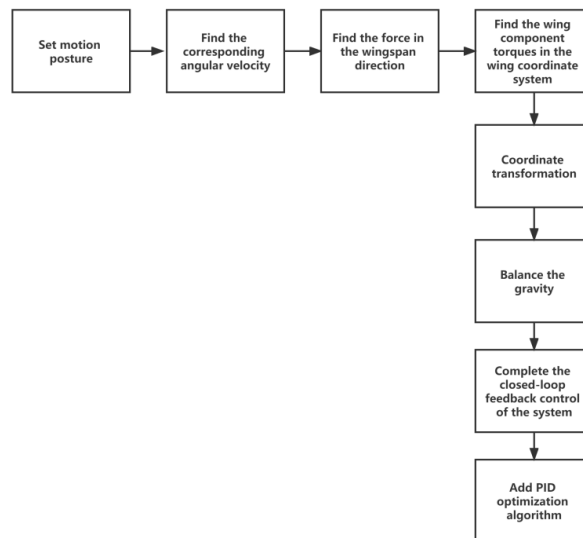


Figure 2: Modeling flow chart

According to the kinetic equation relation (1)- (19) the simulink simulation diagram using the simulink in MATLAB software is shown in Figure 3, and the insect size parameter is [2]:

Table 1: The parameter setting table

parameter	value
Aircraft weight	$1.96 \times 10^{-5} \text{N}$
Wing weight	$2.4 \times 10^{-6} \text{g}$
Wing length	0.3cm
Wing area	0.058cm^2
mean chord	0.097cm
Wing rotation inertia I_x	0.721gcm^2
Wing rotation inertia I_y	0.069gcm^2
Wing rotation inertia I_z	0.148gcm^2

The initial value of attitude angle is set: ϕ is 10° and θ is 20° and ψ is 30° . The following figure is a simulation diagram of flapping aircraft:

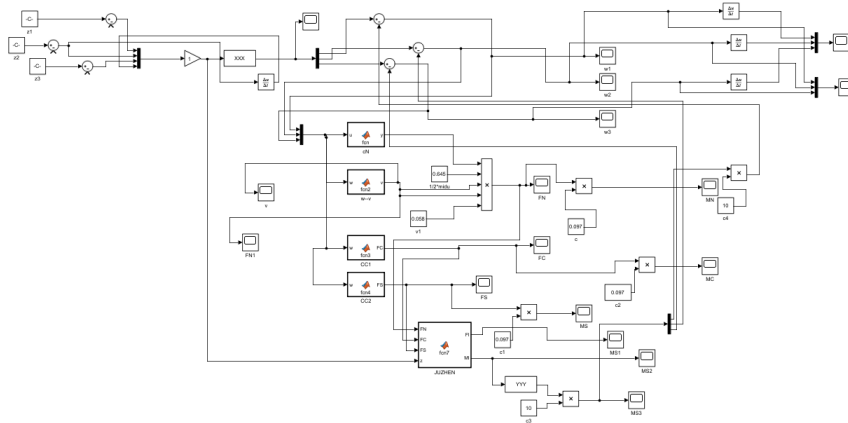


Figure 3: Simulation diagram of dynamic modeling

3.1 Model analysis under no PID control

The aircraft size parameters are shown in Table 1 and the simulation calculation shows that the components of the three angular speeds of the insect are shown in Fig. 4:

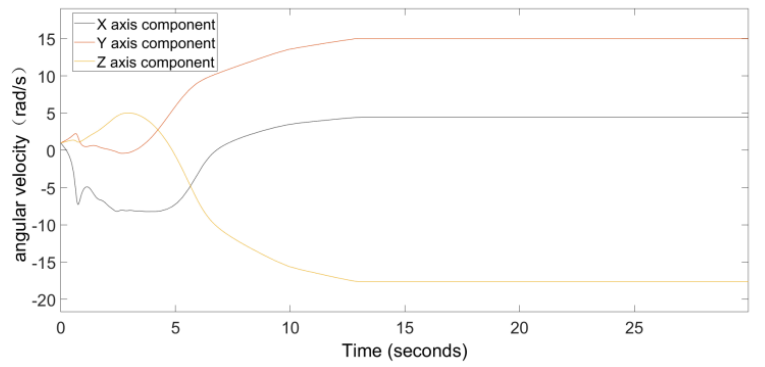


Figure 4: The angular velocity component diagram of the aircraft

After a certain period of adjustment, each component of the insect velocity was stabilized at 13S. Because the aircraft has to overcome gravity first, and then at the final stability, the Z axis angular

velocity produces torque and gravitational moment is used to offset the X axis and Y axis band torque, corresponding to the Z-axis angular velocity from the highest value of + 5.03 rad/s change-17.6rad/s.The X-axis stability value is 14.98rad/s; the Y-axis stability value is 4.43 rad/s.

In this process, they change greatly and not gently, and their rate of change is:

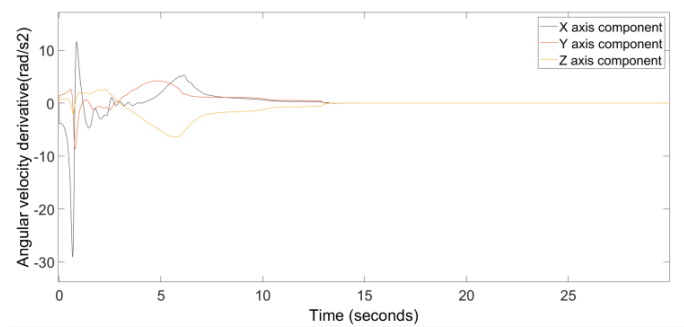


Figure 5: Varplot of angular velocity

It can see that the curves in the figure fluctuate greatly, and the triaxes are mutated at the beginning of the simulation. The peak of the rate is large, in which the X axis is the most prominent, the absolute value of the mutation was to 3.98 at the beginning, the highest value of the X axis reached 29.07, and the process is not gentle. At 13.65s, all three axis components became stable.

3.2 Analysis of the model results after taking the PID control

The control system adopts PID control and adds a PID controller at the front end of the model.

First, consider that the range of start change can not be too large, otherwise the aircraft will not be stable in real conditions when startup. Secondly, giving D too large value above 0.01 will also make the system change rate too large to be easily realized. Giving I the value of more than 0.01 will increase the angular velocity with a rate of change of close to but not less than zero. After a comprehensive comparison, the PID parameters can finally be modulated.

The improvement of change in its three directions is the figure below:

The x-axis is as follows, where the blue line is the improved response curve, the following:

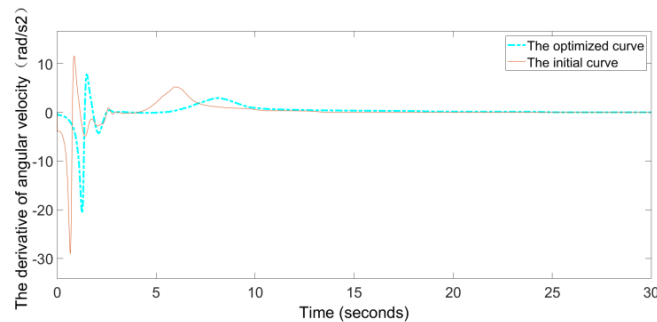


Figure 6: The x-axis components and the optimized comparison diagram

The y-axis ratio of change components and the optimization results are as follows:

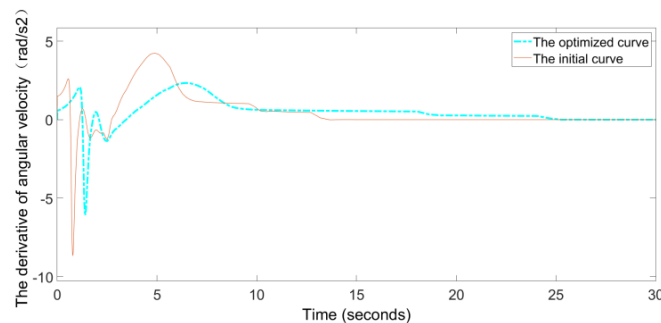


Figure 7: The y-axis components and the optimized comparison plots

The z-axis components and the optimization results are shown in the figure 8 below:

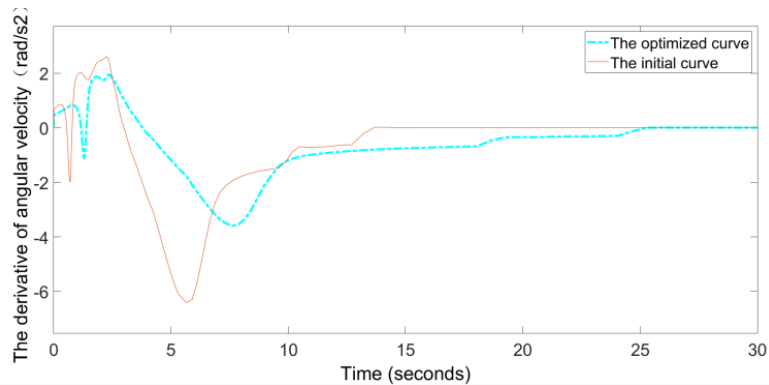


Figure 8: z-axis components and the optimized comparison diagram

This means that the total curve is:

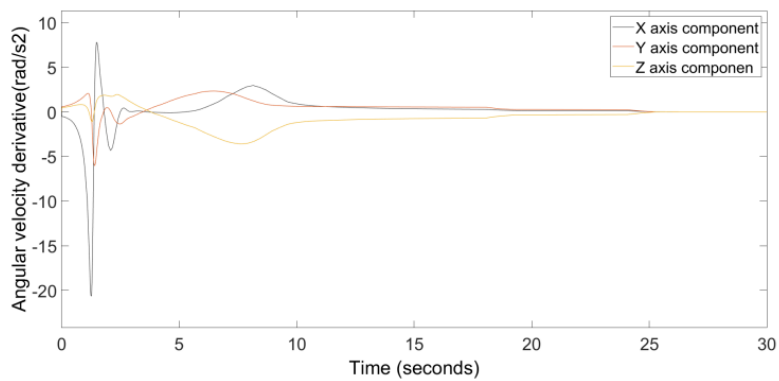
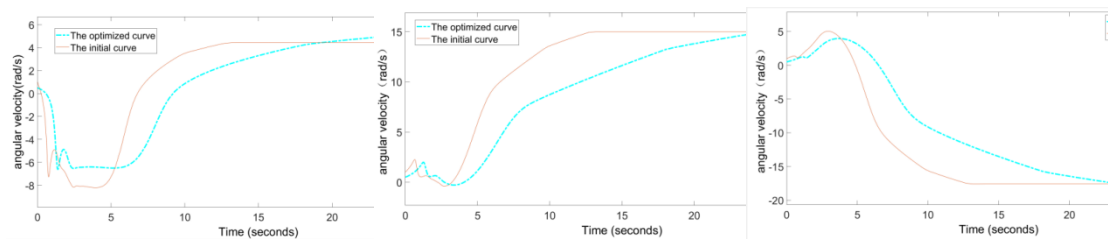


Figure 9: Each component diagram after optimization

At this time, the angular speed of the aircraft decreases, more stable than before: At the beginning of the X-axis optimization, the maximum value of the absolute fluctuation peak value during the process was decreased from 29.07 to 20.64, decreasing by 28.1%; After the Y-axis optimization, the mutation amplitude was reduced by 56.2%, and the maximum peak amplitude was decreased by 30.4%; The Z axis optimized the mutation amplitude by 34% and the maximum peak by 44.0%.

The curve comparing the angular velocity of the three components is:



(a) Comparison of X - axis angular velocity before and after optimization

(b) Comparison of Y - axis angular velocity before and after optimization

(c) Comparison of Z - axis angular velocity before and after optimization

Figure 10: Comparison of optimization effects of each component of angular velocity

At this time, the angular speed change of the aircraft is more gentle, and the peak amplitude decreases.

The fluctuation amplitude of the X-axis was reduced by 21.7%, the final stability value was changed from 4.436 to 5.038, and the stability time was changed from 13.2s to 24.65s;

The fluctuation amplitude of the Y axis is reduced by 44.4%, and the final stability value is constant, but the stability time slows down from 12.71s to 24.64s.

The fluctuation amplitude of the Z-axis was reduced by 31.1%, and the final stability value was constant, but the stability time also slowed, changing from 13.2s to 23.65s. The overall response slows down, and the performance is more stable

4. Conclusion

In this paper, the rigid body dynamics modeling method is used firstly to analyze the wing motion, establish the dynamic model of the wing vehicle,

And then the PID control model is used to control the hovering motion state of the wing aircraft, and control simulation using Simulink. The results show:

(1) After using PID optimization control, the angular velocity fluctuation decreased by 21.7% in X direction amplitude, 44.4% in y direction amplitude and 31.7% compared with that before control;

(2) Using PID optimization control, the angular velocity change rate decreased by 28.1% in x-direction, 56.2% in y-direction, and 30.4% in z-direction.

Finally, the model is more stable, meets the control requirements, and meets the experimental expectations.

References

- [1] He Wei, Ding Shiqiang, Sun Changyin. *Progress in Modeling and Control of Wing Aircraft [J]. Journal of Automation*, 2017,43 (5): 685-696.
- [2] Chen Wenyuan, Zhang Weiping *micro-flapping wing bionic aircraft [M]. Shanghai Jiao Tong University Press*, 2010: 51-59
- [3] Ma Dongfu, Song Bifeng, Xuan Jianlin, et al. *Progress in independent take-off and landing technology of imitation bird flapping wing aircraft [J]. NASA Journal*, 2021,42 (3): 265-273. DOI: 10.3873/j.issn.1000-1328.2021.03.001.
- [4] Zhang Zhijun, Chen Mo, Yang Hejian, et al. *Analysis of the wing aerodynamic characteristics based on XFlow [J]. Journal of Northeastern University (Natural Science Edition)*, 2021,42 (6): 821-828. DOI: 10.12068/j.issn.1005-3026.2021.06.010..
- [5] Ye Jintao, Liu Fengli, Hao Yongping, et al. *Design and analysis of an ultra-low aircraft [J]. Engineering Design Journal*, 2021,28 (4): 473-479. DOI:10.3785/j.issn.1006-754X.2021.00. 052.
- [6] Hu Qingqing, Zhou Xiangdong, Wei Ruixuan, et al. *Full decoupling control [J]. Robots*, 2009, 31 (2): 151-158,165. DOI: 10.3321/j.issn:1002-0446.2009.02.009.
- [7] Zhang Hongzhi, Song feng, Sun CSL, et al. *Review and Prospect of PRS [J]. Aeronautical Journal*, 2021, 42(2): 74-95. DOI: 10.16383/j.aas.2017. c160581
- [8] Su Progress, Fang Zongde, Liu Lan. *General design and experiment of Microflapping Wing Aircraft [J]. Optical Precision Engineering*, 2008,16 (4): 656-661. DOI: 10.3321/j.issn: 1004-924X.2008.04. 015.
- [9] Hu Qingqing, Wei Ruixuan, Cui Xiaofeng, et al. *Study on pose stabilization of imitation bird flapping wing aircraft [J]. Robots*, 2008,30 (6): 481-485. DOI: 10.3321/j.issn: 1002-0446.2008.06.001